

Dependence of exciton transition energy of single-walled carbon nanotubes on surrounding dielectric materials

Y. Miyauchi^a, R. Saito^b, K. Sato^b, Y. Ohno^c, S. Iwasaki^c, T. Mizutani^c, J. Jiang^d, S. Maruyama^{a*}

^aDepartment of Mechanical Engineering, The University of Tokyo, Tokyo 113-8656, Japan

^bDepartment of Physics, Tohoku University and CREST, Sendai 980-8578, Japan

^cDepartment of Quantum Engineering, Nagoya University, Nagoya 464-8603, Japan and

^dCenter for High Performance Simulation and Department of Physics,
North Carolina State University, Raleigh, North Carolina 27695-7518, USA

(Dated: April 11, 2007)

We theoretically investigate the dependence of exciton transition energies on dielectric constant of surrounding materials. We make a simple model for the relation between dielectric constant of environment and a static dielectric constant describing the effects of electrons in core states, σ bonds and surrounding materials. Although the model is very simple, calculated results well reproduce experimental transition energy dependence on dielectric constant of various surrounding materials.

PACS numbers: 78.67.Ch; 78.67.-n; 71.35.-y

I. INTRODUCTION

Photoluminescence (PL) of single-walled carbon nanotubes (SWNTs) has been intensively studied for elucidating their unusual optical and electronic properties due to one dimensionality¹⁻¹⁶. Since both of electron-electron repulsion and electron-hole binding energies for SWNTs are considerably large compared with those for conventional three-dimensional materials, the Coulomb interactions between electron-electron and electron-hole play an important role in optical transition of SWNTs¹⁷⁻²². Optical transition energies of SWNTs are strongly affected by the change of environment around SWNTs such as bundling²³, surfactant suspension^{7,14,24} and DNA wrapping²⁵. Lefebvre *et al.*⁷ reported that the transition energies for suspended SWNTs between two pillars fabricated by the MEMS technique are blue-shifted relative to the transition energies for micelle-suspended SWNTs. Ohno *et al.*¹⁴ have compared the PL of suspended SWNTs directly grown on a grated quartz substrate using alcohol CVD technique⁶ with SDS-wrapped SWNTs². The energy differences between air-suspended and SDS-wrapped SWNTs depend on (n, m) and type of SWNTs [type I $((2n+m) \bmod 3 = 1)$ or type II $((2n+m) \bmod 3 = 2)$ ²⁶⁻²⁸].

Recently, Ohno *et al.* studied E_{11} transition energies of SWNTs in various surrounding materials with different dielectric constant, κ_{env} ²⁹. Observed dependence of E_{11} on κ_{env} for a (n, m) nanotube showed a tendency that can be roughly expressed as

$$E_{11} = E_{11}^{\infty} + A_{nm}^{\text{exp}} \kappa_{\text{env}}^{-\alpha} \quad (1)$$

where E_{11}^{∞} denotes a transition energy when κ_{env} is infinity, A_{nm}^{exp} is the maximum value of an energy change

of E_{11} by κ_{env} , and α is a fitting coefficient in the order of 1, respectively. At this stage, the reason why the experimental curve follows Eq.(1) is not clear.

In the previous theoretical studies of excitonic transition energies for SWNTs^{17,19,21,22}, a screening effect of a surrounding material is mainly described using a static dielectric constant κ . However, since κ consists of both κ_{env} and screening effect by nanotube itself, κ_{tube} , experimental dependence of transition energies on dielectric constants of environment can not directly compared with calculations^{17,19,21,22} using the static dielectric constant κ . In this study, we make a simple model for the relation between κ_{env} and κ . The calculated results of excitons for different κ_{env} reproduced well the experimental transition energy dependence on dielectric constant of various surrounding materials.

II. THEORETICAL METHOD

A. Exciton transition energy

Within the extended tight-binding model^{21,22,28}, we calculated transition energies from the ground state to the first bright exciton state by solving the Bethe-Salpeter equation,

$$\left\{ [E(\mathbf{k}_c) - E(\mathbf{k}_v)] \delta(\mathbf{k}'_c, \mathbf{k}_c) \delta(\mathbf{k}'_v, \mathbf{k}_v) + K(\mathbf{k}'_c \mathbf{k}'_v, \mathbf{k}_c \mathbf{k}_v) \right\} \Psi^n(\mathbf{k}_c \mathbf{k}_v) = \Omega_n \Psi^n(\mathbf{k}'_c \mathbf{k}'_v), \quad (2)$$

where \mathbf{k}_c and \mathbf{k}_v denote wave vectors of the conduction and valence energy bands and $E(\mathbf{k}_c)$ and $E(\mathbf{k}_v)$ are the quasi-electron and quasi-hole energies, respectively. Ω_n is the energy of the n -th excitation of the exciton ($n = 0, 1, 2, \dots$), and $\Psi^n(\mathbf{k}_c \mathbf{k}_v)$ are the excitonic wavefunctions. The kernel $K(\mathbf{k}'_c \mathbf{k}'_v, \mathbf{k}_c \mathbf{k}_v)$ describes the Coulomb interaction between an electron and a hole. Details of the exciton calculation procedure is the same as presented in Refs^{21,22,28}.

*Corresponding author. FAX: +81-3-5841-6421.
E-mail: maruyama@photon.t.u-tokyo.ac.jp (S. Maruyama)

The exciton wavefunction $|\Psi_{\mathbf{q}}^n\rangle$ with a center-of-mass momentum $\mathbf{q}(=\mathbf{k}_c - \mathbf{k}_v)$ can be expressed as

$$|\Psi_{\mathbf{q}}^n\rangle = \sum_{\mathbf{k}} Z_{\mathbf{k}_c, (\mathbf{k}-\mathbf{q})_v}^n c_{\mathbf{k}_c}^+ c_{(\mathbf{k}-\mathbf{q})_v} |0\rangle, \quad (3)$$

where $Z_{\mathbf{k}_c, (\mathbf{k}-\mathbf{q})_v}^n$ is the eigenvector of the n -th ($n = 0, 1, 2, \dots$) state of the Bethe-Salpeter equation, and $|0\rangle$ is the ground state. Due to momentum conservation, the photon-excited exciton is an exciton with $\mathbf{q} \approx 0$ for parallel excitations to the nanotube axis. In this Letter, we calculate the $n = 0$ state of $\mathbf{q} = 0$ exciton for each (n, m) SWNT.

B. Dielectric screening effect

In our calculation, the unscreened Coulomb potential V between carbon π orbitals is modeled by the Ohno potential¹⁹. We consider the dielectric screening effect within the random phase approximation (RPA). In the RPA, the static screened Coulomb interaction W is expressed as¹⁷

$$W = V/\kappa\epsilon(\mathbf{q}), \quad (4)$$

where $\epsilon(\mathbf{q})$ is the dielectric function describing effects of the polarization of the π bands. κ is a static dielectric constant describing the effects of electrons in core states, σ bonds, and surrounding materials. In the calculation, we directly calculate only the polarization for the π band, and the effects of electrons in core states, σ bands, and surrounding materials are represented by a single constant κ . In the most accurate expression, the inhomogeneous and nonlocal dielectric response of the nanotube itself and the surrounding materials should be considered. However, it is not easy within extended tight binding method. In this study, instead of treating the complicated dielectric response including surrounding materials, we make a simple model for a relation between the static dielectric constant κ and κ_{env} to obtain the E_{11} dependence on κ_{env} .

C. Relationship between κ and κ_{env}

Figure 1 shows a schematic view for the model relationship between κ and κ_{env} . Here we consider the screening effect related to κ as a linear combination of the screening of nanotube itself and the surrounding material

$$\frac{1}{\kappa} = \frac{C_{\text{tube}}}{\kappa_{\text{tube}}} + \frac{C_{\text{env}}}{\kappa_{\text{env}}}, \quad (5)$$

where κ_{tube} is the dielectric constant within a nanotube except for the π bands, and C_{tube} and C_{env} are coefficients for the inside and outside of a nanotube, respectively. As shown in Eq.(1), the transition energies observed in the experiment²⁹ indicate that there is a

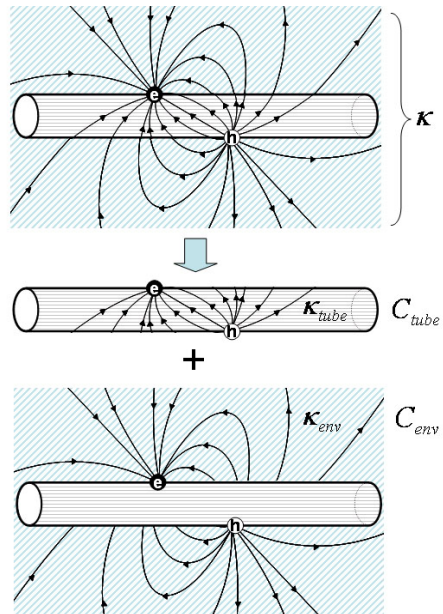


FIG. 1: Schematic of the connection of the net dielectric constant κ and the dielectric constant of the surrounding material κ_{env} and the nanotube itself κ_{tube}

limit value¹⁹ when $\kappa_{\text{env}} \rightarrow \infty$. Hence, when $\kappa_{\text{env}} \rightarrow \infty$, $C_{\text{env}}/\kappa_{\text{env}}$ can be removed from Eq.(5), and $1/\kappa$ is expressed by the limit value as

$$\frac{1}{\kappa} = \frac{C_{\text{tube}}}{\kappa_{\text{tube}}} \equiv \frac{1}{\kappa_{\text{tube}}^{\infty}}, (\kappa_{\text{env}} \rightarrow \infty) \quad (6)$$

where $\kappa_{\text{tube}}^{\infty}$ is the limit value of the net dielectric constant κ when κ_{env} is infinity. Since electric flux lines through inside of the nanotube remain even when $\kappa_{\text{env}} \rightarrow \infty$, we assume there is a certain value of κ ($\kappa_{\text{tube}}^{\infty}$) that corresponds to the situation when dielectric screening by surrounding material is perfect and only dielectric response of the nanotube itself contributes to the net screening effect.

Replacing $C_{\text{tube}}/\kappa_{\text{tube}}$ by $\kappa_{\text{tube}}^{\infty}$, Eq.(5) is modified as

$$\frac{1}{\kappa} = \frac{1}{\kappa_{\text{tube}}^{\infty}} + \frac{C_{\text{env}}}{\kappa_{\text{env}}}. \quad (7)$$

Next, we imagine that the SWNT is placed in the vacuum, which corresponds to $\kappa = \kappa^{\text{vac}}$ and $\kappa_{\text{env}} = 1$, and then C_{env} can be expressed as

$$C_{\text{env}} = \frac{1}{\kappa^{\text{vac}}} - \frac{1}{\kappa_{\text{tube}}^{\infty}}, \quad (8)$$

where κ^{vac} is the static dielectric constant *not* for the vacuum, but for the situation that the nanotube is placed in the vacuum. We now express κ as a function of κ_{env} through two parameters $\kappa_{\text{tube}}^{\infty}$ and κ^{vac} , whose values can be estimated from the following discussions. In the previous papers^{17,19,21,22}, κ value is put around 2 to obtain a

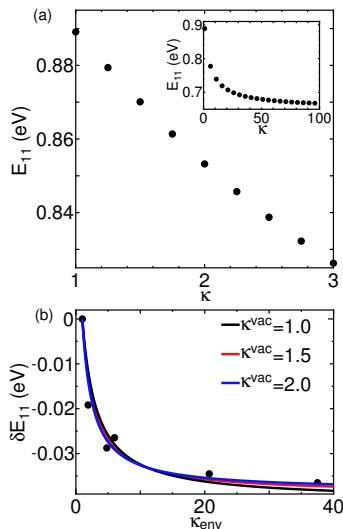


FIG. 2: (a) The E_{11} energy for a (9,8) SWNT as a function of κ . (b) δE_{11} dependence on κ_{env} . Inset in (a) shows the E_{11} dependence up to $\kappa = 100$. In (b), circles denote the experimental data and solid curves denote the calculated results of Eq.(10) for $\kappa^{\text{vac}} = 1.0$ (black), 1.5 (red) and 2.0 (blue).

good fit with experiments for SWNTs with surrounding materials. Jiang *et al.*²¹ have compared the calculated results with the results for the two photon absorption experiments¹⁰, and obtained the best fit using $\kappa = 2.22$ for SWNTs in a polymer matrix. Here, since κ^{vac} is for nanotubes without surrounding materials, κ^{vac} should be less than about 2 and close to 1 due to vacancy of inside of the tubes. With regard to $\kappa_{\text{tube}}^{\infty}$, according to the experimental results^{7,14,29}, transition energy change due to change of surrounding materials is at most 30-100meV. Fig.2(a) shows the calculated E_{11} energy dependence on κ for a (9,8) SWNT in a small κ region, while the inset shows the E_{11} dependence up to $\kappa_{\text{env}} = 100$. As shown in Fig.2(a), variation of κ that yields the transition energy change of 30 to 100 meV is about 1 to 3 when κ is around 2. Therefore, the value of $\kappa_{\text{tube}}^{\infty}$ should be around 2 to 3 and that of κ^{vac} should be around 1 to 2.

D. Dependence of excitation energy on κ_{env}

As shown in Fig.2(a), the calculated E_{11} energies decrease with increasing κ . This is mainly due to the fact that the self energy (e-e repulsion) always exceeds to the e-h binding energy and that the both interactions (e-e and e-h) decrease with increasing κ . The E_{11} almost linearly depends on κ around the small κ region. We checked that the linear dependence is universal for all (n, m) 's for diameters more than 0.7 nm. Assuming the linear dependence, variation of the excitation energy $\delta E_{11} \equiv E_{11} - E_{11}(\kappa_{\text{env}} = 1)$ for the small κ region is approximated by

$$\delta E_{11} = -A_{nm}(\kappa - \kappa^{\text{vac}}), \quad (9)$$

where A_{nm} is the gradient of δE_{11} near the small κ region for each (n, m) type. After we transform κ using the relationship of Eq.(5), Eq.(9) is modified as

$$\delta E_{11} = -A_{nm}(\kappa_{\text{tube}}^{\infty} - \kappa^{\text{vac}}) \left(\frac{\kappa_{\text{env}} - 1}{\kappa_{\text{env}} + (\kappa_{\text{tube}}^{\infty} - \kappa^{\text{vac}})/\kappa^{\text{vac}}} \right). \quad (10)$$

$A_{nm}(\kappa_{\text{tube}}^{\infty} - \kappa^{\text{vac}})$ corresponds to the maximum value of δE_{11} when $\kappa_{\text{env}} \rightarrow \infty$, which corresponds to the value of coefficient A_{nm}^{exp} in the fitting curve of Eq.(1). For (9,8) SWNT, the fitted value to the calculated results for A_{nm} is 33 meV and A_{nm}^{exp} obtained by the fit to the experiment²⁹ using Eq.(1) is 36 meV, and $\kappa_{\text{tube}}^{\infty} - \kappa^{\text{vac}}$ should be around 1. The values for $\kappa_{\text{tube}}^{\infty}$ and κ^{vac} are consistent with the values conventionally used for SWNTs in dielectric materials^{17,19,21,22}.

III. RESULTS AND DISCUSSION

Figure 2(b) compares δE_{11} for a (9,8) SWNT depending on κ_{env} by the experiment (solid circles) and the calculated results (lines) for $\kappa^{\text{vac}} = 1, 1.5, 2.0$ using Eq.(10). As shown in Fig.2(b), the qualitative shape of theoretical curves are in good agreement with the experiment and not affected so much by the change of κ^{vac} . Since the exact value of κ^{vac} is unknown, we hereafter set $\kappa^{\text{vac}} = 1.5$ for each (n, m) SWNT. For the (9,8) SWNT in Fig.2(b), $\kappa_{\text{tube}}^{\infty} = 2.7$ and $\kappa^{\text{vac}} = 1.5$ are fitting values. These values are consistent with the discussion in the previous section. After setting $\kappa^{\text{vac}} = 1.5$, Eq.(10) turns to be

$$\delta E_{11} = \frac{-A_{nm}(\kappa_{\text{env}} - 1)}{\kappa_{\text{env}}/(\kappa_{\text{tube}}^{\infty} - \kappa^{\text{vac}}) + 1/1.5}. \quad (11)$$

Thus, we express δE_{11} as a function of κ_{env} with one parameter $(\kappa_{\text{tube}}^{\infty} - \kappa^{\text{vac}})$.

Figure 3(a) shows the calculated values of A_{nm} for each (n, m) 's. Family pattern of $(2n + m = \text{const.})$ family is drawn with the $2n + m$ values by dotted lines. We found a slight diameter dependence and relatively large chiral angle dependence of A_{nm} for type II SWNTs (blue) compared with type I SWNTs (red). The type II SWNTs with larger chiral angles tend to have larger value of A_{nm} . For a convenient use of Eq.(10), we give a fitting function of A_{nm} meV as

$$A_{nm} = A + Bd_t + (C + D/d_t) \cos 3\theta, \quad (12)$$

which gives the average (maximum) error of $\pm 2\text{meV}$ (8meV) for type I, and $\pm 2\text{meV}$ (5meV) for type II SWNTs. The fit curve is shown in Fig.3(a) by solid lines. Here d_t (nm) is the diameter of nanotube and θ is the chiral angle²⁶. The values of (A, B, C, D) are (36, -4, 0, 0) and (33, -3, 6, 7) for type I and for type II SWNTs, respectively.

In order to expand our result to many (n, m) SWNTs, we need a function to describe $(\kappa_{\text{tube}}^{\infty} - \kappa^{\text{vac}})$. It is important to note that $\kappa_{\text{tube}}^{\infty}$ should depend on the diameter.

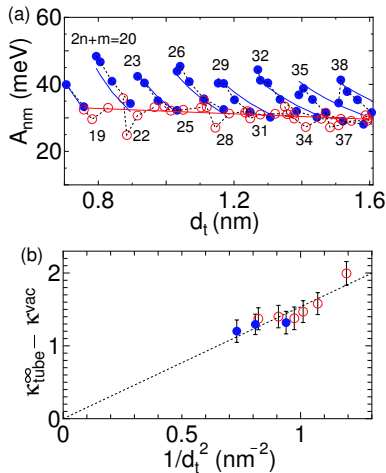


FIG. 3: (a) Calculated values of A_{nm} for each (n, m) SWNT. Open (red) and solid (blue) circles correspond to type I and type II SWNTs, respectively. Solid lines denote the fit curve by Eq.(12). (b) $\kappa_{\text{tube}}^{\infty} - \kappa^{\text{vac}}$ vs $1/d_t^2$. The values of $\kappa_{\text{tube}}^{\infty} - \kappa^{\text{vac}}$ are obtained by the fit of Eq.(10) to the experimental data for each (n, m) .

An exact function should be calculated by taking into account the Coulomb interaction considering induced surface charge at the boundary of the nanotube and surrounding material for an e-e or e-h pair for each (n, m) SWNT. Instead of calculating this complicated function, here we roughly estimate the $(\kappa_{\text{tube}}^{\infty} - \kappa^{\text{vac}})$ as a simple function of diameter d_t , since $(\kappa_{\text{tube}}^{\infty} - \kappa^{\text{vac}})$ should depend on the cross section of a SWNT. As shown in Fig.3(b), $(\kappa_{\text{tube}}^{\infty} - \kappa^{\text{vac}})$ is roughly proportional to $1/d_t^2$,

$$(\kappa_{\text{tube}}^{\infty} - \kappa^{\text{vac}}) = \frac{E}{d_t^2}, \quad (13)$$

with the coefficient $E = 1.5 \pm 0.3 \text{ nm}^2$. Here $(\kappa_{\text{tube}}^{\infty} - \kappa^{\text{vac}})$ is obtained by the fit using Eq.(10) and A_{nm} calculated for each chirality. Fig.3(b) clearly shows that our calculated A_{nm} well describes the chiral angle dependence of δE_{11} and that the remaining diameter dependence is understood by $(\kappa_{\text{tube}}^{\infty} - \kappa^{\text{vac}})$ through $1/d_t^2$. This $1/d_t^2$ dependence implies that $\kappa_{\text{tube}}^{\infty}$ depends on the volume of inner space of the nanotube. Although the number of experimental data available for the fit is small and selection of this function is arbitrary to some extent, it is reasonable that $1/\kappa_{\text{tube}}^{\infty}$ increase with the increase of the diameter, since $1/\kappa_{\text{tube}}^{\infty}$ corresponds to the Coulomb interaction through the inner space of the nanotube. In order to find an accurate form of the function, future experiments and theoretical studies are definitely needed.

Figure 4 shows δE_{11} as a function of κ_{env} for (a) the experiment and (b) the calculation using Eq.(11) and (13). Fig.4(c) compares δE_{11} for the experiment and that for the calculation with the same κ_{env} values. The same symbols for an (n, m) are used in three figures of Fig.4. Details of experimental data will be published elsewhere²⁹. Although our treatment is very simple, the calculated

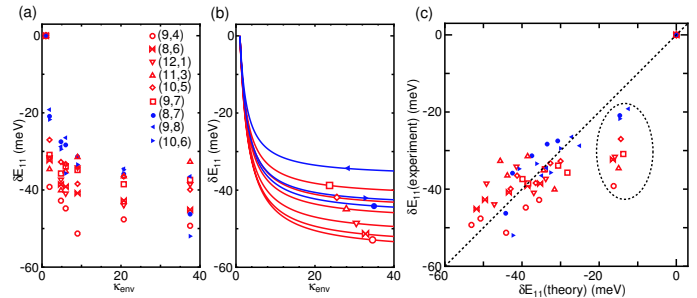


FIG. 4: The transition energy dependence plotted as a function of κ_{env} . (a) experiment and (b) calculated results are indicated by (a) symbols and (b) solid curves. In (b), (n, m) for each curve is indicated by a symbol on the curve. (c) Comparison of δE_{11} for the experiment ($\delta E_{11}(\text{experiment})$) and calculation ($\delta E_{11}(\text{theory})$). A dotted line indicates the line of $\delta E_{11}(\text{experiment}) = \delta E_{11}(\text{theory})$. Open (red) and solid (blue) symbols correspond to type I and type II SWNTs, respectively. The data in the dotted circle are the data for $\kappa_{\text{env}} = 1.9$ ²⁹ (see text).

curves for various (n, m) SWNTs well reproduce the experimentally observed tendency for each (n, m) SWNT, and the degree of difference between each (n, m) type is also in good agreement with the experiment. As shown in Fig.4(c), $\delta E_{11}(\text{theory})$ is in a good agreement with $\delta E_{11}(\text{experiment})$ except for several points indicated by a dotted circle in the figure, which correspond to a case for the smallest $\kappa_{\text{env}} = 1.9$ (hexane) except for $\kappa_{\text{env}} = 1$ (air) in the experimental data²⁹. The value of $\kappa_{\text{env}} = 1.9$ for hexane is adopted as the dielectric constant for the material, in which the dipole moments of liquid hexane are not aligned perfectly even in the presence of the electric field. Since $\kappa_{\text{env}} = 1.9$ is a macroscopic value, a local dielectric response might be different from the averaged macroscopic response. If the local dielectric constant near SWNTs becomes large (for example, $\kappa_{\text{env}} \approx 3$), the fitting of Fig.4(c) becomes better. We expect that the dipole moments of a dielectric material might be aligned locally for a strong electric field near an exciton, which makes the local dielectric constant relatively large. This will be an interesting subject for exciton PL physics. Since the difference of A_{nm} between each (n, m) type decreases with increasing the diameter, it is predicted that the amount of variation due to the change of κ_{env} mostly depend on diameter in the larger diameter range. Thus a PL experiment for nanotubes with large diameters would be desirable for a further comparison.

IV. SUMMARY

In summary, the dependence of exciton transition energies on dielectric constant of surrounding materials are investigated. We proposed a model for the relation between dielectric constant of the environment and a static dielectric constant κ in the calculation. Although the

model is quite simple, calculated results well reproduce the feature of experimentally observed transition energy dependence on dielectric constant of various surrounding materials, and various d_t and θ .

Grant-in-Aid (No. 16076201) from the Ministry of Education, Japan.

Acknowledgments

Y.M. is supported by JSPS Research Fellowships for Young Scientists (No. 16-11409). R.S. acknowledges a

-
- ¹ M. J. O'Connell, S. M. Bachilo, X. B. Huffman, V. C. Moore, M. S. Strano, E. H. Haroz, K. L. Rialon, P. J. Boul, W. H. Noon, C. Kittrell, J. Ma, R. H. Hauge, R. B. Weisman, R. E. Smalley, *Science* 297 (2002) 593.
- ² S. M. Bachilo, M. S. Strano, C. Kittrell, R. H. Hauge, R. E. Smalley, R. B. Weisman, *Science* 298 (2002) 2361.
- ³ S. Lebedkin, K. Arnold, F. Hennrich, R. Krupke, B. Renker, M. M. Kappes, *New J. Phys.* 5 (2003) 140.
- ⁴ S. M. Bachilo, L. Balzano, J. E. Herrera, F. Pompeo, D. E. Resasco, R. B. Weisman, *J. Am. Chem. Soc.* 125 (2003) 11186.
- ⁵ A. Hartschuh, H. N. Pedrosa, L. Novotny, T. D. Krauss, *Science* 301 (2003) 1354.
- ⁶ Y. Miyauchi, S. Chiashi, Y. Murakami, Y. Hayashida, S. Maruyama, *Chem. Phys. Lett.* 387 (2004) 198.
- ⁷ J. Lefebvre, J. Fraser, Y. Homma, P. Finnie, *Appl. Phys. A* 78 (2004) 1107.
- ⁸ F. Wang, G. Dukovic, L. E. Brus, T. F. Heinz, *Science* 308 (2005) 838.
- ⁹ J. Maultzsch, R. Pomraenke, S. Reich, E. Chang, D. Prezzi, A. Ruini, E. Molinari, M. S. Strano, C. Thomsen, C. Lienau, *Phys. Rev. B* 72 (2005) 241402.
- ¹⁰ G. Dukovic, F. Wang, D. Song, M. Y. Sfeir, T. F. Heinz, L. E. Brus, *Nano Lett.* 5 (2005) 2314.
- ¹¹ S. G. Chou, F. Plentz Filho, J. Jiang, R. Saito, D. Nezich, H. B. Ribeiro, A. Jorio, M. A. Pimenta, G. G. Samsonidze, A. P. Santos, M. Zheng, G. B. Onoa, E. D. Semke, G. Dresselhaus, M. S. Dresselhaus, *Phys. Rev. Lett.* 94 (2005) 127402.
- ¹² H. Htoon, M. J. O'Connell, S. K. Doorn, V. I. Klimov, *Phys. Rev. Lett.* 94 (2005) 127403.
- ¹³ F. Plentz, H. B. Ribeiro, A. Jorio, M. S. Strano, M. A. Pimenta, *Phys. Rev. Lett.* 95 (2005) 7401.
- ¹⁴ Y. Ohno, S. Iwasaki, Y. Murakami, S. Kishimoto, S. Maruyama, T. Mizutani, *Phys. Rev. B* 73 (2006) 235427.
- ¹⁵ Y. Miyauchi, S. Maruyama, *Phys. Rev. B* 74 (2006) 35415.
- ¹⁶ Y. Miyauchi, M. Oba, S. Maruyama, *Phys. Rev. B* 74 (2006) 205440.
- ¹⁷ T. Ando, *J. Phys. Soc. Jpn.* 66 (1997) 1066.
- ¹⁸ H. Zhao, S. Mazumdar, *Phys. Rev. Lett.* 93 (2004) 157402.
- ¹⁹ V. Perebeinos, J. Tersoff, P. Avouris, *Phys. Rev. Lett.* 92 (2004) 257402.
- ²⁰ C. D. Spataru, S. Ismail-Beigi, L. X. Benedict, S. G. Louie, *Phys. Rev. Lett.* 92 (2004) 077402.
- ²¹ J. Jiang, R. Saito, G. G. Samsonidze, A. Jorio, S. G. Chou, G. Dresselhaus, M. S. Dresselhaus, *Phys. Rev. B* 75 (2007) 035407.
- ²² J. Jiang, R. Saito, K. Sato, J. S. Park, G. G. Samsonidze, A. Jorio, G. Dresselhaus, M. S. Dresselhaus, *Phys. Rev. B* 75 (2007) 035405.
- ²³ C. Fantini, A. Jorio, M. Souza, M. S. Strano, M. S. Dresselhaus, M. A. Pimenta, *Phys. Rev. Lett.* 93 (2005) 147406.
- ²⁴ V. C. Moore, M. S. Strano, E. H. Haroz, R. H. Hauge, R. E. Smalley, *Nano Lett.* 3 (2003) 1379.
- ²⁵ D. A. Heller, E. S. Jeng, T.-K. Yeung, B. M. Martinez, A. E. Moll, J. B. Gastala, M. S. Strano, *Science* 311 (2006) 508.
- ²⁶ R. Saito, G. Dresselhaus, M. S. Dresselhaus, *Physical Properties of Carbon Nanotubes*, Imperial College Press, London, 1998.
- ²⁷ A. Jorio, C. Fantini, M. A. Pimenta, R. B. Capaz, G. G. Samsonidze, G. Dresselhaus, M. S. Dresselhaus, J. Jiang, N. Kobayashi, A. Grüneis, R. Saito, *Phys. Rev. B* 71 (2005) 075401.
- ²⁸ G. G. Samsonidze, R. Saito, N. Kobayashi, A. Grüneis, J. Jiang, A. Jorio, S. G. Chou, G. Dresselhaus, M. S. Dresselhaus, *Appl. Phys. Lett.* 85 (2004) 5703.
- ²⁹ Y. Ohno, S. Iwasaki, Y. Murakami, S. Kishimoto, S. Maruyama, T. Mizutani, arXiv:0704.1018v1 [cond-mat.mtrl-sci] (2007).